# Layer-Structured Poly(vinyl alcohol)/Graphene Oxide Nanocomposites with Improved Thermal and Mechanical Properties

**Xiaoming Yang,[1,2] Songmin Shang,[2] Liang Li[2,3]**

[1]*College of Chemistry, Chemical Engineering and Materials Sciences, Soochow University, Suzhou 215123, People's Republic of China*
[2]*Institute of Textiles and Clothing, The Hong Kong Polytechnic University, Hong Kong, People's Republic of China*
[3]*Key Laboratory for Green Chemical Process of Ministry of Education, School of Materials Science and Engineering, Wuhan Institute of Technology, Wuhan, People's Republic of China*

Received 6 March 2010; accepted 12 August 2010
DOI 10.1002/app.33279
Published online 23 November 2010 in Wiley Online Library (wileyonlinelibrary.com).

**ABSTRACT:** Layer-structured poly(vinyl alcohol)/graphene oxide nanocomposites in the form of films are prepared by simple solution processing. The structure and properties of these nanocomposites are studied using X-ray diffractions, scanning electron microscopy, Fourier-transform infrared spectroscopy, differential scanning calorimetry, and thermogravimetric analysis. The results indicate that graphene oxide is dispersed on a molecular scale and aligned in the poly(vinyl alcohol) matrix, and there exists strong interfacial interactions between both components, which are responsible for the significant improvement in the thermal and mechanical properties of the nanocomposites. © 2010 Wiley Periodicals, Inc. J Appl Polym Sci 120: 1355–1360, 2011

**Key words:** nanocomposites; mechanical properties; thermal properties

## INTRODUCTION

Polymer-based nanocomposites are the subject of increased interest in the last decades because of their enhanced properties arising from the reinforcement of fillers.[1–3] Especially, when the properties depend on the surface area of the fillers, small amounts (typically less than 5%) of nanosized fillers give rise to the same level of mechanical and thermal improvements as are typically achieved with loadings of 30–50% of microsized fillers.[4] Clay minerals and carbon nanostructures have been proposed as candidates for the nanofillers.[5–7] The dispersion of the nanofillers within the polymer matrix has significant influence on the properties of the composites. If the nanofillers in the polymer matrix could be dispersed on a molecular scale and interacted with the matrix by chemical bonding or strong intermolecular interactions, significant improvements in the thermal and mechanical properties of the nanocomposites or unexpected new properties might be achieved.

Recently, a two-dimensional single-layered graphene oxide (GO) has attracted a great deal of attention because of its low cost, unique structure, and remarkable properties.[8–10] There are various oxygen functional groups (e.g., hydroxyl, epoxide, and carbonyl groups) attached on the basal planes and edges of GO sheets. Thus, GO is hydrophilic and capable of forming stable colloidal suspensions as individual sheets in water. Meanwhile, these oxygen-containing groups impart GO sheets with the function of strong interaction with polar small molecules or polymers to form GO-intercalated or -exfoliated composites.[11–16] Therefore, by combining extraordinary properties and low cost, it is expected for two-dimensional GO sheets to be used as promising nanoscaled filler for the next generation of nanocomposite materials.[17,18] Inspired from those studies, this work is focused on investigating the properties of poly(vinyl alcohol) (PVA)/GO nanocomposites. PVA is water soluble, nontoxic, and highly hydrophilic, with wide industrial applications in paper coating,

*Correspondence to:* X. Yang (yangxiaoming@suda.edu.cn) or L. Li (msell08@163.com)

Contract grant sponsor: The Hong Kong Polytechnic University; contract grant number: 4-ZZ63.
Contract grant sponsor: Key Project in Science and Technology Innovation Cultivation Program of Soochow University.
Contract grant sponsor: Educational Bureau of Hubei Province; contract grant number: Q20091508.
Contract grant sponsor: Scientific Research Foundation for Returned Overseas Chinese Scholars of MOE; contract grant number: [2009]1341.
Contract grant sponsor: Scientific Research Key Project of MOE; contract grant number: 209081.
Contract grant sponsor: National Natural Science Foundation of China; contract grant number: 20904044.

textile sizing, and flexible packaging films. These applications stimulate an interest in improving thermal and mechanical properties of thin PVA films by the fabrication of PVA nanocomposite films.

In this study, layer-structured PVA/GO nanocomposites were prepared by incorporating GO into a PVA matrix using a simple solution processing method. We investigate the effects of GO loading on the properties of PVA/GO nanocomposites. The properties of the nanocomposites are studied in the film form as a function of GO content in the matrix polymer. GO content of the nanocomposites is varied from 0 to 3.5 wt %. We also examine the relationship between the properties and structures of the PVA/GO nanocomposite films.

## EXPERIMENTAL

### Materials

PVA (99+% hydrolyzed, $M_w \sim$ 89,000–98,000) was purchased from Aldrich (America). Graphite powder was purchased from Uni-Chem (Hong Kong, China). Other reagents were of analytical grade and used without further purification.

### Synthesis of hybrid materials

GO was prepared from graphite by the modified Hummers method.[19,20] PVA/GO nanocomposites with 0.5, 1, 2, and 3.5 wt % of filler were prepared as follows: GO was dissolved in 10 mL of water and treated with ultrasound for 45 min to make a homogenous brown dispersion (1 mg/mL). PVA powder was dissolved in distilled water at 90°C, and the solution was subsequently cooled to room temperature. The GO aqueous dispersion was gradually added to the PVA solution and sonicated at room temperature for 30 min to obtain homogeneous PVA/GO solutions. Finally, the above solutions were allowed to stand overnight to remove air bubbles, then poured into glass dishes, and kept at 40°C for film formation until its weight equilibrated.

### Characterization

X-ray diffraction (XRD) patterns were obtained using a PHILIPS PW 3710 diffractometer using Cu Kα radiation source (λ = 1.5418 Å) at room temperature. Fourier-transform infrared (FTIR) spectra were recorded on a Perkin–Elmer spectrum 100 FTIR spectrometer with a 4 $cm^{-1}$ resolution. The glass-transition and crystallization behaviors were investigated by differential scanning calorimetry using a Perkin–Elmer Pyris 1 in nitrogen atmosphere. The samples were heated from room temperature to 240°C, maintained at this temperature for 5 min, then cooled to room temperature, and heated again to 240°C. The heating and cooling rates were 10°C/min in all cases. Thermogravimetric analysis (TGA) was carried out on a Netzch STA 449C instrument at a heating rate of 10°C/min in an air atmosphere. The failure surfaces of the PVA/GO nanocomposite films (after tensile tests) were observed via scanning electron microscopy (SEM; JEOL Model JSM-6490). The failure surfaces were coated with gold before analysis. The tensile strength, elongation, and modulus of PVA/GO nanocomposites were measured on a universal tensile testing machine (Instron 4411) at 20°C with 60% relative humidity. The extension rate was 5 mm/min, and the load cell was 250 N, with a gauge length of 40 mm. The specimen dimension was 60 mm in length, 10 mm in width, and 0.04 mm in thickness. Five parallel measurements were carried out for each sample.

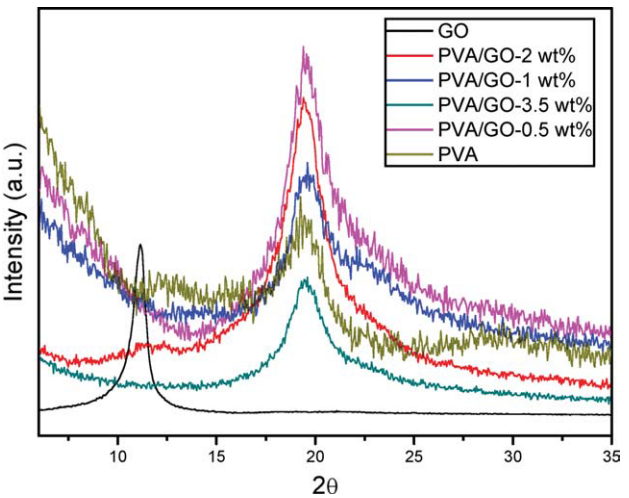


**Figure 1** XRD patterns of GO, PVA and PVA/GO nanocomposite. [Color figure can be viewed in the online issue, which is available at wileyonlinelibrary.com.]

## RESULTS AND DISCUSSION

Figure 1 shows the XRD patterns of pure GO, pure PVA (curve b), and PVA/GO nanocomposite. The characteristic XRD peak of pure GO sheets appears at 2θ = 11.1°, corresponding to a *d*-spacing of 0.78 nm.[21] It indicates that GO is successfully synthesized from graphite powder by a modified Hummers method. PVA shows diffraction peak at 19.5°, which corresponds to the crystalline phase of the polymer.[22] However, for the PVA/GO nanocomposite, its XRD pattern only shows the PVA diffraction peak from PVA and the diffraction peak of GO disappears. This clearly demonstrates the disappearance of the regular and periodic structure of graphene, the formation of fully exfoliated structures, and the homogeneous distribution of GO sheets in the polymer matrix.[23]

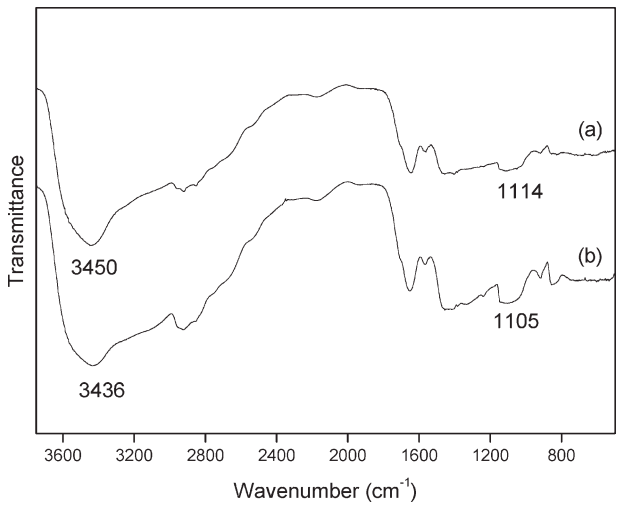


**Figure 2** FTIR spectra of (a) PVA and (b) PVA/2 wt % GO nanocomposite.

To characterize the nanocomposites and to determine the interaction between polymer matrix and the nanofillers, FTIR experiments were performed. It is well known that both the -OH stretching and the -C-OH stretching bands are sensitive to the hydrogen bonding. As shown in Figure 2, the band around 3600–3300 $cm^{-1}$, involving the strong hydroxyl band for free and hydrogen bonded alcohols, is broadened and shifts to a lower wavenumber when GO nanofillers is added into the PVA matrix. This could be attributed to the dissociation of the hydrogen bonding among the hydroxyl groups in the polymer.[24] Another similar change in the FTIR spectrum of the PVA/GO nanocomposite is also observed for the band corresponding to the -C-OH stretching at about 1100 $cm^{-1}$, indicating hydrogen bonding between the -OH in PVA and the oxygenated groups in GO nanofillers.[24,25]

**TABLE I**
**Glass-Transition Temperature and Melting Parameters of PVA and PVA/GO Nanocomposites**

| Samples | $T_g$ (°C) | $T_m$ (°C) | $\Delta H$ (J/g) | $X_c$ (%) |
|---|---|---|---|---|
| PVA | 76 | 228 | 53.1 | 38.3 |
| PVA/0.5 wt % GO | 78 | 228 | 52.6 | 37.9 |
| PVA/1 wt % GO | 79 | 228 | 51.7 | 37.0 |
| PVA/2 wt % GO | 82 | 228 | 52.1 | 37.6 |
| PVA/3.5 wt % GO | 84 | 226 | 39.9 | 28.8 |

The glass-transition and melting behavior of the polymer matrix in the nanocomposites were also investigated. The transition temperatures and melting enthalpy were taken from the second heating run in the calorimetric curves. As shown in Figure 3 and Table I, with the addition of GO in the nanocomposites, the glass-transition temperature ($T_g$) of PVA increases gradually from 76°C to 84°C (Fig. 4), which can be explained by the reduced mobility of polymer chains.[26] The increase in $T_g$ indicates an effective attachment of PVA in the vicinity of the surface of the GO nanosheets, which constrains the segmental motion of the PVA chains by hydrogen bonding.[2,20,27] The degree of crystallinity ($X_c$) is calculated from the ratio of $\Delta H/\Delta H_0$, which are the measured and the 100% crystalline melting enthalpy, respectively. The melting enthalpy of a 100% crystalline PVA, $\Delta H_0$, is taken as 138.6 J/g.[28] The crystallinity of PVA in the nanocomposites is determined by considering the weight fraction of PVA in the nanocomposites. For the crystallization of PVA, there are no obvious changes in the melting temperature ($T_m$) and melting enthalpy ($\Delta H$) when the GO content is below 2 wt %, as reported by others.[29,30] In our case, when the GO content is increased to 3.5 wt %, the

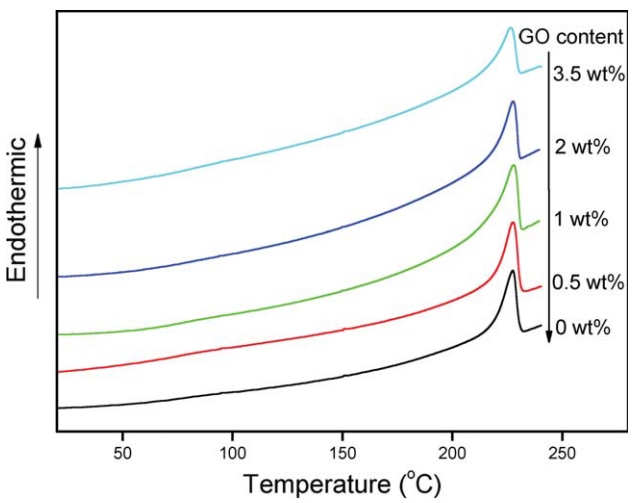


**Figure 3** Differential scanning calorimetry traces of PVA and PVA/GO nanocomposites. [Color figure can be viewed in the online issue, which is available at wileyonlinelibrary.com.]

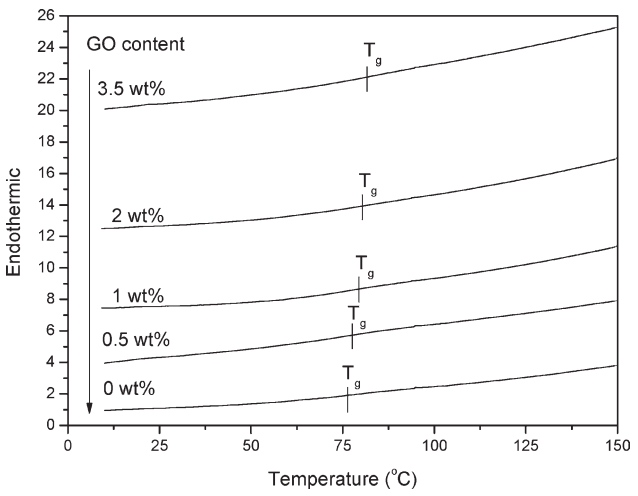


**Figure 4** Higher resolution of differential scanning calorimetry traces of PVA and PVA/GO nanocomposites.

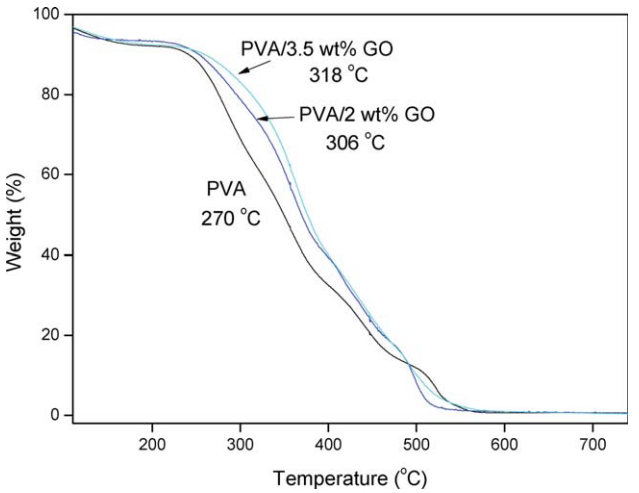


**Figure 5** TGA curves of (a) PVA, (b) PVA/2 wt % GO, and (c) PVA/3.5 wt % GO nanocomposites. [Color figure can be viewed in the online issue, which is available at wileyonlinelibrary.com.]

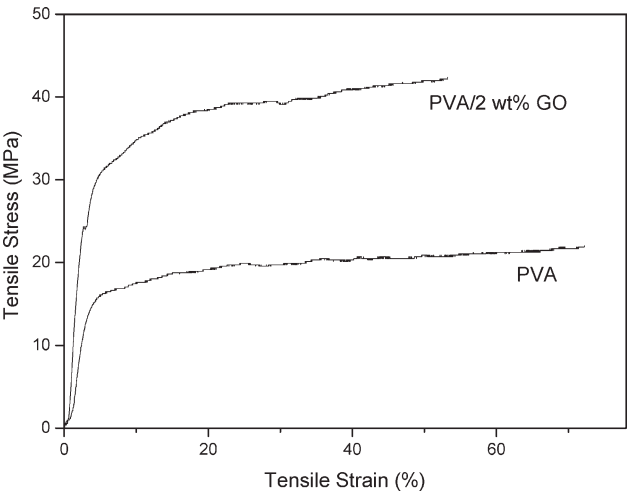


**Figure 6** Typical stress–strain behaviors for the films of pure PVA and PVA/2 wt % GO nanocomposite.

crystallinity of PVA decreases to some extent, suggesting the existence of more interaction between the polymer and the filler to the detriment of interactions among polymer chains to suppress the crystallization of PVA.[31]

Thermal stability represents one of the most important properties in polymer nanocomposites. As shown in Figure 5, TGA is further used to characterize the thermal properties of PVA/GO nanocomposites. The temperature of the maximum degradation rate for the nanocomposites (obtained from the derivative of TGA curves) is increased by about 30–40°C in comparison with that of pure PVA. These results indicate that the mobility of the polymer segments at the interfaces of PVA and GO is suppressed by strong interactions, which improves the thermal stability of PVA.[25]

The homogeneous dispersion of nanofillers in the matrix and the strong interaction between them are beneficial not only to improve thermal property but also to enhance mechanical property of the nanocomposites. In our case, the mechanical performance of the PVA/GO nanocomposite is significantly increased compared with that of the pure PVA matrix, as shown in Table II. The elongation at break of the nanocomposite films gradually decreases with increasing GO content. The typical stress–strain curves of PVA and PVA/2 wt % GO nanocomposite films are presented in Figure 6. The tensile stress and modulus increase sharply by 92.2% from 22 to 42 MPa and by 167% from 0.45 to 1.21 GPa, respectively, with the increase in GO loading from 0 to 2 wt %. Furthermore, when 3.5 wt % or more of GO was added, the nanocomposite films showed more brittle failure (Table I), which is probably caused by the aggregation of nanofillers in the nanocomposite films.[32] The reinforcement effect can be quantitatively evaluated by measuring the increasing rates of modulus and tensile stress at low GO volume content for PVA/GO nanocomposites.[33,34] It has been reported that the mechanical properties of a ductile polymer composite with two-dimensional nanofillers have linear relationships with the volume contents of fillers on the basis of a simple shear lag model.[33] As shown in Figure 7, tensile stress and modulus of

**TABLE II**
**Tensile Properties of Pure PVA and PVA/GO Nanocomposite Films**

| Samples | Tensile stress (MPa) | Modulus (GPa) | Tensile strain (%) |
|---|---|---|---|
| PVA | 22 ± 1 | 0.45 ± 0.2 | 72 ± 6 |
| PVA/0.5 wt % GO | 30 ± 2 | 0.59 ± 0.3 | 66 ± 5 |
| PVA/1 wt% GO | 37 ± 2 | 0.72 ± 0.5 | 57 ± 4 |
| PVA/2 wt % GO | 42 ± 3 | 1.21 ± 0.7 | 53 ± 4 |
| PVA/3.5 wt % GO | 32 ± 2 | 1.46 ± 0.8 | 16 ± 2 |

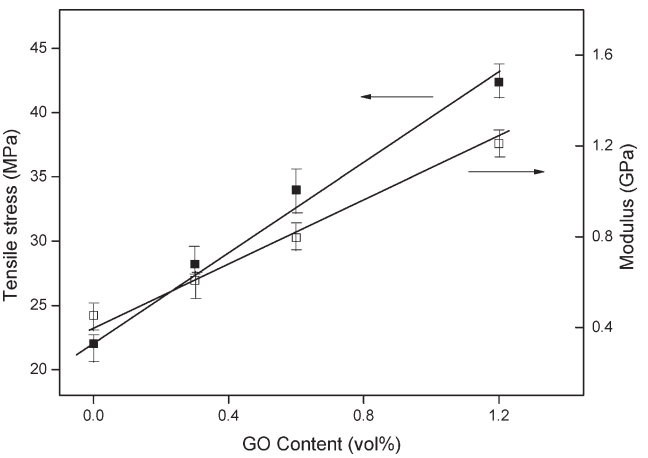


**Figure 7** Tensile stress and modulus of the PVA/GO composite films as a function of volume fraction of GO.

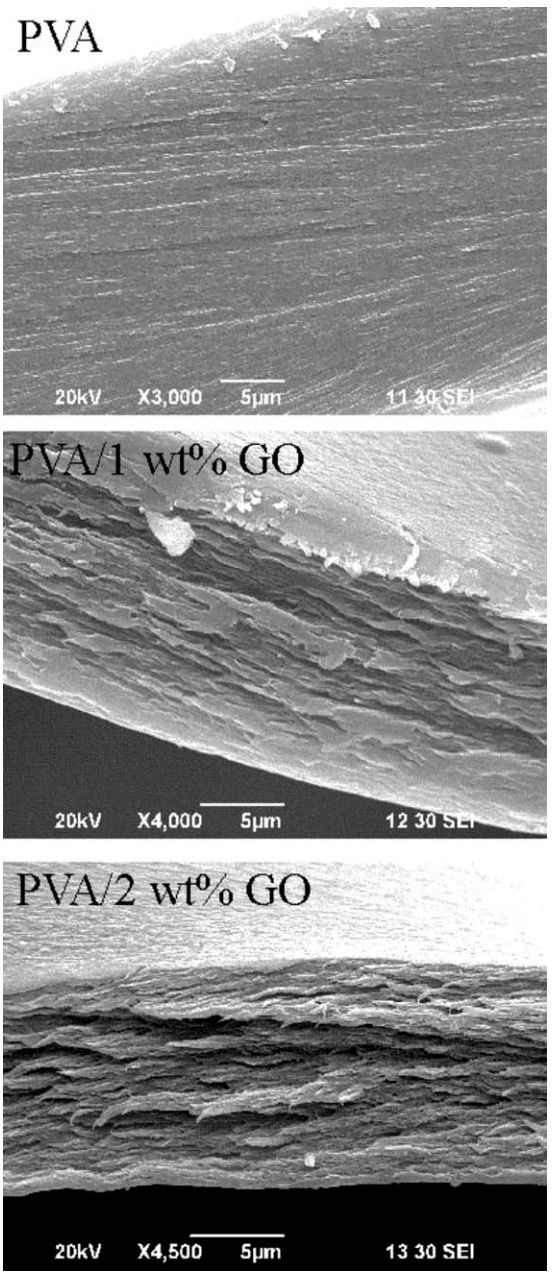


**Figure 8** SEM images of the fracture surface of PVA, PVA/1 wt % GO, and PVA/2 wt % GO nanocomposites.

the nanocomposites increase almost linearly with the volume content of GO, and the corresponding increasing rates were fitted to be 1.8 ± 0.3 and 86 ± 11 GPa, respectively. These reinforcement values are close to those of PVA/carbon nanotubes composites.[34] After the addition of 0.8 wt % functioned carbon nanotubes into the PVA matrix, the tensile modulus increased by 79% (from 2.4 to 4.3% GPa), and the tensile yield strength increased by 47% (from 73 to 107 MPa). The elongation at break significantly decreased, indicating the composites became somewhat more brittle compared with pure PVA.[2]

These results demonstrate that the enhancement of mechanical properties of the PVA/GO nanocomposites could be ascribed to the uniform dispersion on a molecular scale and alignment of GO in the polymer matrix and strong interfacial interactions between both components.

Because PVA is a semicrystalline polymer, its mechanical properties should strongly depend on the degree of its crystallinity. However, as shown in Figure 3 and Table I, no obvious change in PVA crystallinity is observed in PVA/GO nanocomposites containing 2 wt % GO. Therefore, the significant increase in the stress and modulus of the PVA/GO nanocomposites cannot be ascribed to the changes in PVA crystallinity. Thus, it is reasonable to attribute the significant improvement of mechanical properties for the nanocomposites to the homogeneous dispersion of GO sheets in the polymer matrix and strong interfacial interactions between both components. Similar results have been observed for polymer/carbon nanotubes nanocomposites.[35]

The strength of interfacial interactions between the polymer matrix and GO sheets are further investigated by examining the fracture surfaces by using SEM as shown in Figure 8. The SEM micrograph of pure PVA is characterized with smooth surface. On the other hand, the fracture surfaces of the PVA/GO films after tensile testing are totally different from that of the pure PVA, in which the surface is affected by the exfoliation of GO sheets. They are also different with those of the films of the polymer/carbon nanotubes composites.[36] It is characterized by the hybrid structure, which appears gradually as separated parallel layers in the case of the nanocomposites with the addition of GO, just like that of the GO membranes.[8,37] It suggests that the water-dispersed GO and PVA assemble into a layer-stacking macroscopic structure.

## CONCLUSIONS

A simple solution processing method to produce PVA/GO nanocomposites with layered structure has been reported. The film of the PVA/2 wt % GO nanocomposite is strong and ductile. Its modulus and tensile stress are 167% and 92.2% higher than those of pure PVA. On the basis of the results, the improved thermal and mechanical properties of the nanocomposites are mainly due to the homogeneous dispersion and alignment of GO in PVA matrix and the interactions between both components. It demonstrates that GO can be used effectively as a two-dimensional reinforcement nanofiller to prepare polymer nanocomposites with high performance.

## References

1. Li, J.; Vaisman, L.; Marom, G.; Kim, J. K. Carbon 2007, 45, 744.
2. Liu, L. Q.; Barber, A. H.; Nuriel, S.; Wagner, H. D. Adv Funct Mater 2005, 15, 975.

3. Hamming, L. M.; Qiao, R.; Messersmith, P. B.; Brinson, L. C. Comp Sci Technol 2009, 69, 1880.
4. Strawhecker, K. E.; Manias, E. Chem Mater 2000, 12, 2943.
5. Darder, M.; Colilla, M.; Ruiz-Hitzky, E. Chem Mater 2003, 15, 3774.
6. Quan, H.; Zhang, B. Q.; Zhao, Q.; Yuen, R. K. K.; Li, R. K. Y. Compos Part A 2009, 40, 1506.
7. Coleman, J. N.; Khan, U.; GunKo, K. Adv Mater 2006, 18, 689.
8. Dikin, D. A.; Stankovich, S.; Zimney, E. J.; Piner, R. D.; Dommett, G. H. B.; Evmenenko, G.; Nguyen, S. T.; Ruoff, R. S. Nature 2007, 448, 457.
9. Gomez-Navarro, C.; Burghard, M.; Kern, K. Nano Lett 2008, 8, 2045.
10. Guo, H. L.; Wang, X. F.; Qian, Q. Y.; Wang, F. B.; Xia, X. H. ACS Nano 2009, 3, 2653.
11. Verdejo, R.; Barroso-Bujans, F.; Rodriguez-Perez, M. A.; Sajab, J. A.; Lopez-Manchado, M. A. J Mater Chem 2008, 18, 2221.
12. Du, X.; Yu, Z. Z.; Dasari, A.; Ma, J.; Mo, M.; Meng, Y.; Mai, Y. W. Chem Mater 2008, 20, 2066.
13. Yang, Y.; Wang, J.; Zhang, J.; Liu, J.; Yang, X.; Zhao, H. Langmuir 2009, 25, 11808.
14. Matsuo, Y.; Tahara, K.; Sugie, Y. Carbon 1997, 35, 113.
15. Han, Y.; Lu, Y. Comp Sci Technol 2009, 69, 1231.
16. Liu, P. G.; Gong, K. C.; Xiao, P.; Xiao, M. J Mater Chem 2000, 10, 933.
17. Kotov, N. A.; Dekany, I.; Fendler, J. H. Adv Mater 1996, 8, 637.
18. Xu, J.; Hu, Y.; Song, L.; Wang, Q.; Fan, W.; Chen, Z. Carbon 2002, 40, 450.
19. Hummers, W. S.; Offeman, R. E. J Am Chem Soc 1958, 80, 1339.
20. Ramanathan, T.; Abdala, A. A.; Stankovich, S.; Dikin, D. A.; Herrera-Alonso, M.; Piner, R. D.; Adamson, D. H.; Schniepp, H. C.; Chen, X.; Ruoff, R. S.; Nguyen, S. T.; Aksay, I. A.; Prudhomme, R. K.; Brinson, L. C. Nat Nanotechnol 2008, 3, 327.
21. Ni, Z. H.; Wang, H. M.; Kasim, J.; Fan, H. M.; Yu, T.; Wu, Y. H.; Feng, Y. P.; Shen, Z. X. Nano Lett 2007, 7, 2758.
22. Garcia-Cerda, L. A.; Escareno-Castro, M. U.; Salazar-Zertuche, M. J Non-Cryst Solids 2007, 353, 808.
23. Du, X. S.; Xiao, M.; Meng, Y. Z.; Hay, A. S. Carbon 2005, 43, 195.
24. Lu, L. Y.; Sun, H. L.; Peng, F. B.; Jiang, Z. Y. J Membr Sci 2006, 281, 245.
25. Matsuo, Y. Hatase, K.; Sugie, Y. Chem Mater 1998, 10, 2266.
26. Mbhele, Z. H.; Salemane, M. G.; Sittert, C.; Nedeljkovic, J. M.; Djokovic, V.; Luyt, A. S. Chem Mater 2003, 15, 5019.
27. Yao, Z. L.; Braidy, N.; Botton, G. A.; Adronov, A. J Am Chem Soc 2003, 125, 16015.
28. Su, J. X.; Wang, Q.; Su, R.; Wang, K.; Zhang, Q.; Fu, Q. J Appl Polym Sci 2008, 107, 4070.
29. Liang, J.; Huang, Y.; Zhang, L.; Wang, Y.; Ma, Y.; Guo, T.; Chen, Y. Adv Funct Mater 2009, 19, 2297.
30. Xu, Y.; Hong, W.; Bai, H.; Li, C.; Shi, G. Carbon 2009, 47, 3538.
31. Salavagione, H. J.; Martinez, G.; Gomez, M. A. J Mater Chem 2009, 19, 5027.
32. Alla, S. G. A.; El-Din, H. M. N.; El-Naggar, A. W. M. J Appl Polym Sci 2006, 102, 1129.
33. Bonderer, L. J.; Studart, A. R.; Gauckler, L. J. Science 2008, 319, 1069.
34. Coleman, J. N.; Khan, U.; Blau, W. J.; Gunko, Y. K. Carbon 2006, 44, 1624.
35. Zhang, X. F.; Liu, T.; Sreekumar, T. V.; Kumar, S.; Moore, V. C.; Hauge, R. H.; Smalley, R. E. Nano Lett 2003, 3, 1285.
36. Wang, S. F.; Shen, L.; Zhang, W. D.; Tong, Y. J. Biomacromolecules 2005, 6, 3067.
37. Chen, C.; Yang, Q. H.; Yang, Y.; Lv, W.; Wen, Y.; Hou, P. X.; Wang, M.; Cheng, H. M. Adv Mater 2009, 21, 3007.